On Optimal Downlink Coverage in Poisson Cellular Networks with Power Density Constraints

Tharaka Samarasinghe, *Member, IEEE,* Hazer Inaltekin, *Member, IEEE,* and Jamie S. Evans, *Member, IEEE*

***Abstract*—This paper studies downlink coverage maximization for cellular networks in which base station (BS) locations are modeled using a spatial Poisson point process, considering three different coverage models, and under constraints on transmit power, BS density and transmit power density. Firstly, the coverage optimization problem is solved analytically for the first coverage model that focuses on noise-limited communication by ignoring interference and random fading effects. This model provides useful insights into the significance of bounded path loss models to obtain meaningful solutions for this problem. The other two coverage models are based on the users' received signal-to-interference-plus-noise-ratio (SINR) from their associated BSs. For these models, it is shown that the coverage optimization problem can be reduced to a constrained single dimensional optimization problem without any loss of optimality. The related solutions can be obtained with limited computational complexity by resorting to a numerical search over a compact subset of candidate values. Bounds on the optimum BS density are also provided to further truncate the search space. All results are derived for general bounded path loss models. Specific applications are also illustrated to provide further design insights and to highlight the importance of using bounded path loss models for coverage analysis.**

***Index Terms*—Cellular networks, coverage, optimization, Poisson point process, stochastic geometry.**

I. Introduction

A. Background and Motivation

LOCATION modeling for base stations (BS) is of prime importance for coverage optimization in cellular network analysis and planning. Conventionally, BS locations were considered to be fixed when abstracting their locations for analytical purposes. These techniques included grid based modeling methods such as the well known hexagonal grid model [1], [2]. However, in most cases, these models lacked analytical tractability, leading to complex system level simulations. Therefore, as an alternative, there has been a continued and increasing research interest in using stochastic geometric based approaches to model BS locations in wireless networks [3], [4]. Unlike grid based models, these techniques consider BS locations as randomly drawn from a spatial stochastic process, with Poisson point processes (PPP) being the most widespread ones [5]. These models are capable of statistically emulating complex heterogeneous networks of today in which BSs are irregularly deployed based on the customer density and network traffic. In this paper, we study coverage maximization for the downlink of such a Poisson cellular network having constraints on the BS transmit power and BS density.

Using stochastic geometry to analyze and design wireless communication networks has been a key area of research in the past decade, *e.g.*, see [3], [5] and the references therein for an overview of work in this area. To name a few, some recent previous work includes analysis of downlink coverage for interfering networks [6]–[8], heterogeneous networks consisting of macro, pico and femto cells [7]–[10], modeling the uplink coverage [11], multiple access interference modeling [12]–[14], multi-antenna networks [9], [15], cooperative networks [16], [17], and random power control [18]. Out of these works, [6] and [7] are the most related ones to this paper as they focus on obtaining expressions for downlink coverage probabilities in interfering Poisson cellular networks.

In this paper, the BS locations are modeled using a homogenous spatial PPP of intensity λ. The signal received by a user is impaired by both path loss and fading. Different from [6] and [7], which consider the classical power-law, *i.e.*, $g(r) = r^{-\alpha}$ for $\alpha > 2$, to characterize the location dependent path loss values of the mobile users, the coverage analysis in this paper is performed for general bounded path loss models that satisfy some mild conditions. We show that using bounded path loss models reveals some underlying important dynamics of the tradeoff between power and BS density, which were otherwise hidden under unbounded power law models. In particular, we show that the *density-invariance property of outage probability* obtained in [6] and [7] is primarily due to the unbounded nature of the path loss model used in these previous works. Hence, the coverage analysis in this paper mainly focuses on bounded path loss models, which are more accurate for small scale transmitter-receiver separations and asymptotically decay as a power-law at large distances.

Another major contribution of this paper is the derivation of coverage maximizing transmit power and BS density values under power density constraints by using coverage probability expressions obtained through stochastic geometry. This is an under-explored research problem in the literature, but an important one with an increasing interest on future green wireless networks. In [19], Cao *et al.* focused on minimizing

Manuscript received June 24, 2013; revised November 20, 2013. The editor coordinating the review of this paper and approving it for publication was O. Oyman.

This work was supported in part by the Australian Research Council under Grant DP-11-0102729, and in part by the European Commission Research Executive Agency Marie Curie FP7-Reintegration-Grants under Grant PCIG10-GA-2011-303713. The material in this paper was presented in part at the Australian Communications Theory Workshop, Adelaide, Australia, January 2013, and at the IEEE Vehicular Technology Conference, Las Vegas, USA, September 2013.

T. Samarasinghe and J. S. Evans are with the Department of Electrical and Computer Systems Engineering, Monash University, Australia (e-mail: {tharaka.samarasinghe, jamie.evans}@monash.edu).

H. Inaltekin is with the Department of Electrical and Electronics Engineering, Antalya International University, Turkey (e-mail: hazeri@antalya.edu.tr).

Digital Object Identifier 10.1109/TCOMM.2014.020814.130470

the BS density of a cellular network operating in an interference limited regime under a probabilistic quality of service constraint on the rate of a generic user. In this paper, different from [19], the transmit power per BS P and the BS density λ function as two main levers to increase or decrease the network coverage probability. We focus on maximizing the network coverage probability under three separate constraints. In particular, we set finite individual constraints on P and λ, *i.e.*, $P \leq P_{\max}$ and $\lambda \leq \lambda_{\max}$. However, since the BSs are modeled as a PPP with an infinite number of BSs in the network, the value of P on its own does not constitute a fair and meaningful metric about the network power expenditure, which is an important performance criterion. Therefore, we also set finite constraints on $P\lambda$ (*i.e.*, $P\lambda \leq \rho$), which can be interpreted as the average transmit power per unit area or the power density. This quantity is also called the average network power consumption [20]. Due to the constraint on the multiplication of P and λ, there is an obvious tradeoff between our design parameters because an upwards increase in one variable leads to a corresponding downwards decrease in the other. Under these constraints, we investigate how λ and P can be set optimally to maximize the downlink network coverage probability for cellular wireless networks. Our contributions are explained in more detail in the following subsection together with the organization of the paper.

B. Contributions and the Organization of the Paper

In Section II, we first introduce the system model, formally define three coverage models, and then formulate the coverage maximization problem for general path loss models. The three coverage models differ from each other depending on the metric used to decide whether a user is in coverage or not. The first model is simple as it neglects interference and random fading effects, and decides on coverage by considering the received unfaded signal-to-noise-ratio (SNR). That is, it assumes that there exists a perfect scheduling scheme among the BSs eliminating interference from nearby transmitters, and we focus on an *almost* deterministic model of wireless networks with the only randomness remaining in BS locations. The other two coverage models are based on the received signal-to-interference-plus-noise-ratio (SINR). In the first SINR-based coverage model, we say a user is covered if the received SINR from its nearest BS is above a given threshold value τ. In the second SINR-based coverage model, we say a user is covered if the maximum received SINR is above τ.

The downlink coverage probability analysis is given in Section III. We obtain expressions for the coverage probability for a generic user in the network, considering each of the coverage models and general path loss models. In particular, we show that the coverage probability is a strictly increasing function of P. Then, we use the derived coverage probability expressions to obtain solutions for the optimization problem of interest in Section IV. We particularly discuss how the optimization problem can be reduced to a constrained single dimensional optimization problem over λ without any loss of optimality, which simplifies the analysis. In particular, this allows us to perform a numerical search over a compact subset of candidate λ values on the $P\lambda = \rho$ curve to find the optimum λ and P with limited computational complexity, regardless of the coverage and path loss models. For the SNR-based coverage model, we solve the downlink coverage maximization problem analytically, and obtain closed form results for specific path loss models. The derived solutions indicate why the bounded nature of the path loss model is important to provide revealing insights about the downlink coverage maximization problem. In contrast to the SNR-based coverage model, obtaining analytical expressions for the optimal values of λ and P for the SINR-based coverage models is relatively more complex, and we resort to a numerical search over a truncated set of candidate λ values on the $P\lambda = \rho$ curve. We further prune off the search space by providing tighter bounds on λ that can be utilized to increase the computational efficiency of the numerical search in cases where $\lambda_{\max}$ is large.

Finally, we apply the derived results in Sections III and IV to a specific bounded path loss model in Section V. After obtaining expressions for the coverage probability for this particular path loss model, we first illustrate how the coverage behaves with different system parameters and the constraints. In particular, we show that the coverage probability first increases with λ up to a threshold value $\lambda^{\star}$ since increasing the density of the BSs decreases the average distance between a user and its associated BS. However, after $\lambda^{\star}$, increasing the BS density further will increase wireless multiple-access interference more dominantly and deteriorate the coverage probability. On the other hand, if the path loss model is unbounded, the coverage probability is strictly increasing with λ. This behavior is a manifestation of the unrealistic singularity at 0 in this path loss model. Due to such a singularity, a user can progressively achieve higher channel power gains without any bound by getting closer and closer to a BS, irrespective of the interference. Therefore, maximizing the BS density in the network maximizes the coverage simultaneously. Also, we show that the density-invariance property of the outage probability established in [6] and [7] can only be expected to hold in sparse wireless networks.

Then, we illustrate how the maximum coverage probability behaves with the power density constraint ρ. This curve can be considered as the Pareto optimal boundary between the power density constraint and the coverage probability. For a particular ρ, any power density-coverage probability pair below the curve is achievable, but suboptimal, whereas the power density-coverage probability pairs above the curve cannot be achieved. In addition, we also illustrate how the coverage maximizing λ and P values change when the constraint on power density is relaxed. In particular, we show that although the coverage can be improved indefinitely by increasing P, it becomes interference limited and cannot be improved indefinitely by increasing λ. Section VI concludes the paper.

II. System Model and Problem Setup

We consider a cellular network with BSs located according to a homogenous spatial PPP Φ of intensity λ. Each BS has a single transmit antenna with a transmit power of P. Mobile users are equipped with single receive antennas, and are located according to an arbitrary configuration over the plane. We assume that there exists a *test* user located at the origin, and we focus on the coverage probability of this user.

This assumption does not limit the generality of our results due to the Slivnyak's theorem [3]–[5].

Consider a BS located at point $x \in \Phi$. The path loss value between the BS at x and the test user at the origin is given by $g(\|x\|)$, where $\|\cdot\|$ represents the Euclidean norm. The path loss model is general in the sense that g can be any function that is continuous, positive, non-increasing, and $g(r) = O\left(r^{-\alpha}\right)$ as r grows large for some $\alpha > 2$. The additive noise is assumed to be Gaussian with zero mean and unit variance. In this setting, $\mathrm{SNR}_x = Pg(\|x\|)$ represents the received unfaded SNR at the test user from a BS located at $x \in \Phi$.

We are interested in the coverage of the test user. To this end, we formally define three coverage models that differ from each other depending on the metric considered when deciding whether a user is in coverage or not. The first coverage model, which we call the SNR-*based coverage model* (SBCM), considers SNR_x to be the decision metric for coverage. We formally define the SBCM as follows.

Definition 1: We say that a user is covered according to the SBCM if the received unfaded SNR from its nearest BS is above a given threshold value τ, *i.e.*, $\mathrm{SNR}_{x^\star} > \tau$, where $x^\star$ is the location of the nearest BS.

In this simple coverage model, we neglect interference when making a decision on coverage. This amounts to assuming that there exists a perfect scheduler distributing all available communication resources (*e.g.,* frequency blocks, time slots and etc.) among the BSs such that concurrent transmissions take place without causing interference to each other. In a more practical sense, it is enough to only consider the communication resources available to the nearby BSs around the test user since the interference coming from the distant BSs will be negligible. Further, we also neglect random fading effects, *i.e.*, we focus on an almost deterministic model of wireless networks, with the only randomness remaining in BS locations.

Next, we focus on networks with interference and fading. The random variable $h_x \sim \exp(1)$ represents the independent and identically distributed (i.i.d.) random Rayleigh fading coefficient for $x \in \Phi$. Therefore, the received instantaneous SINR at the test user from a BS at point x is given by

$$\mathrm{SINR}_x = \frac{Ph_x g(\|x\|)}{1 + \sum_{y \in \Phi \setminus \{x\}} Ph_y g(\|y\|)}. \quad (1)$$

The other two coverage models consider the received SINR for determining whether a user is covered or not, and differ from each other depending on the rules for user-BS association. In the first SINR-based coverage model, the users connect to their nearest BSs for data communication, and therefore we consider the SINR from the nearest BS to be the decision metric when deciding whether a user is in coverage or not. We call this the *Nearest BS Coverage Model* (NBCM), and formally define it as follows.

Definition 2: We say that a user is covered according to the NBCM if the received SINR from its nearest BS is above a given threshold value τ, *i.e.*, $\mathrm{SINR}_{x^\star} > \tau$, where $x^\star$ is the location of the nearest BS.

On the other hand, the second SINR-based coverage model considers the maximum received SINR to be the decision metric when deciding whether a user is in coverage or not. We call it the *Best BS Coverage Model* (BBCM), and formally define it as follows.

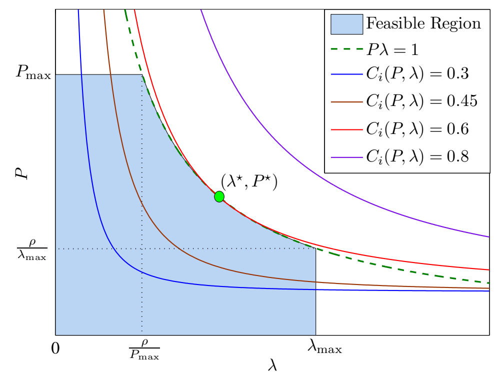

Fig. 1. Graphical representation of the solution to the optimization problem.

Definition 3: We say that a user is covered according to the BBCM if the maximum received SINR is above a given threshold value τ, *i.e.*, $\max_{x\in\Phi} \mathrm{SINR}_x > \tau$.

For the SBCM, it is not hard to see that the BS providing the largest received unfaded SNR turns out to be the nearest BS geographically. Therefore, the user-BS association will be the same.

Let $C_S(P,\lambda) = \Pr\{\mathrm{SNR}_{x^\star} > \tau\}$, $C_N(P,\lambda) = \Pr\{\mathrm{SINR}_{x^\star} > \tau\}$ and $C_B(P,\lambda) = \Pr\{\max_{x\in\Phi} \mathrm{SINR}_x > \tau\}$ be coverage probabilities for the SBCM, NBCM and BBCM, respectively. We are interested in maximizing the coverage probability under constraints on the BS transmit power and the BS density. In particular, we set finite constraints on P and λ. In the analysis, we refer to them as individual constraints on P and λ. Further, we set finite constraints on the $P\lambda$ product, which is a design parameter having the power density interpretation since it represents the average transmit power per unit area. We analyze how to set λ and P optimally to maximize the network coverage probability such that these constraints are not violated. The resulting coverage maximization problem can be written as

$$\begin{array}{ll} \underset{P,\lambda}{\text{maximize}} & C_i(P,\lambda) \\ \text{subject to} & P\lambda \le \rho \\ & 0 \le P \le P_{\max} \\ & 0 \le \lambda \le \lambda_{\max} \end{array}, \quad (2)$$

where $i \in \{S, N, B\}$.

The behavior of $C_i\left(P,\lambda\right)$ and a graphical overview of the structure of candidate solutions to the optimization problem in (2) are illustrated in Fig. 1 through a schematic sketch that roughly illustrates the behavior of the coverage probability. $P\lambda = \rho$ represents a hyperbola in the $P-\lambda$ plane (*i.e.*, the green dashed line in Fig. 1, where we have set $\rho = 1$). Hence, the shaded region, which is the domain enclosed by the hyperbola, and the lines $P = P_{\max}$, $P = 0$, $\lambda = \lambda_{\max}$, and $\lambda = 0$, represents the feasible set of pairs for this optimization problem. The pair providing the highest coverage probability gives us the optimal BS density $\lambda^\star$ and the optimal power $P^\star$. That is, if we plot the contours of $C_i(P,\lambda)$ (the solid lines in the figure) in the $P-\lambda$ plane, we need to find the contour curve having the highest value and intersecting with the feasible region. For this particular example, coverage probabilities of 0.3 and 0.45 can be achieved, but they are sub-optimal since we can find a $(\lambda^{\star}, P^{\star})$ pair in the feasible set that also lies on the higher $C_i(P, \lambda) = 0.6$ contour. Any probability greater than 0.6 cannot be achieved because those contours fall outside of the feasible set, *e.g.*, $C_i(P, \lambda) = 0.8$. Hence, it turns out that 0.6 is the maximum achievable coverage probability for this example. It is interesting to note that the $P\lambda = \rho$ curve will shift to the right when ρ is increased. Therefore, if $\rho \geq P_{\max}\lambda_{\max}$, the feasible region will be the rectangle enclosed by $P = P_{\max}$, $P = 0$, $\lambda = \lambda_{\max}$, and $\lambda = 0$, which implies that the optimization problem will be independent of ρ for this scenario. In the remaining parts of the paper, we will focus on solving the optimization problem in (2) by making use of the guiding principles explained above.

III. Coverage Probability Calculations

In this section, we will focus on the coverage models defined in the previous section, and we will obtain expressions for the coverage probability of a test user at the origin by using key tools from stochastic geometry. The coverage probability expressions will be derived for general path loss models, and these expressions will be instrumental in solving the coverage optimization problem posed in (2). We will start with the simple but insightful coverage model given in Definition 1. In addition to being insightful, this simplified model allows us to analytically solve the optimization problem in (2), which will be presented in Section IV.

A. The SNR*-based Coverage Model (SBCM)*

The coverage probability expression for the SBCM is formally stated in the following lemma.

Lemma 1: For the SBCM, the coverage probability of a user is given by

$$C_S(P, \lambda) = 1 - \mathrm{e}^{-\lambda\pi\left(g^{-1}\left(\frac{\tau}{P}\right)\right)^2}, \tag{3}$$

where $g^{-1}(x) = \inf\{r : g(r) \leq x\}$.

Proof: See Appendix A. ■

B. The Nearest BS Coverage Model (NBCM)

The coverage probability expression for the NBCM is formally stated in the following lemma.

Lemma 2: For the NBCM, the coverage probability of a user is given by

$$C_N(P, \lambda) = \pi\lambda \int_0^{\infty} \exp\left(-q_1(P, \lambda, r)\right) dr, \tag{4}$$

where $q_1(P, \lambda, r) = q_2(P, \lambda, \sqrt{r}) + \lambda\pi r$, and

$$q_2(P, \lambda, r) = \frac{\tau}{Pg(r)} + \lambda \int_{r^2}^{\infty} \frac{\pi\tau g(\sqrt{v})}{g(r) + \tau g(\sqrt{v})} dv.$$

Moreover, if the distance to the nearest BS $\|x^{\star}\|$ is given, the coverage probability is given by $C_N(P, \lambda | \|x^{\star}\|) = \exp\left(-q_2(P, \lambda, \|x^{\star}\|)\right)$.

Proof: See Appendix A. ■

We note that, as a by-product of Lemma 2, we obtain the coverage probability expression for the special case of the NBCM, in which the distance to the nearest BS is given. Although this special case of the NBCM is not very much helpful in solving the optimization problem of interest in this paper, it can still be used to obtain coverage probability expressions for network models where the distance between the user and its associated BS is fixed. For example, we can use this result to study coverage (using general bounded path loss models) in an ad hoc network where the transmitter-receiver pairs are modeled using the well known Poisson bipolar model (PBM) [4], [21], [22].

C. The Best BS Coverage Model (BBCM)

In this coverage model, a user is said to be covered if the maximum of received SINRs from all the BSs is above τ, where $\tau > 1$. The assumption of $\tau > 1$ makes the analysis more tractable because it ensures that only one BS will provide an SINR value above the threshold [7]. This assumption is also common in most existing works that consider the maximum SINR value as a decision variable for scheduling [23]–[25]. Under this assumption, the coverage probability expression for the BBCM is obtained in the following lemma.

Lemma 3: For the BBCM, the coverage probability of a user is given by

$$C_B(P, \lambda) = \pi\lambda \int_0^{\infty} \exp\left(-q_3(P, \lambda, r)\right) dr, \tag{5}$$

where

$$q_3(P, \lambda, r) = \frac{\tau}{Pg(\sqrt{r})} + \lambda \int_0^{\infty} \frac{\pi\tau g(\sqrt{v})}{g(\sqrt{r}) + \tau g(\sqrt{v})} dv.$$

Proof: See Appendix A. ■

It is not hard to see that the coverage expressions obtained in Lemmas 1, 2 and 3 are all strictly increasing functions of P. This is obvious for the SBCM since increasing the transmit power increases the received unfaded SNR. Even for the SINR-based models, increasing the transmit power reduces the effect of noise on the SINR, which can be written as

$$\mathrm{SINR}_x = \frac{h_x g(\|x\|)}{\frac{1}{P} + \sum_{y \in \Phi\setminus\{x\}} h_y g(\|y\|)}.$$

The above expression clearly shows that increasing P decreases the term related to the background noise in the denominator, thus increasing the SINR regardless of the noise power. It can be also seen that the SINR expression will be independent of P irrespective of the path loss model if the noise power is zero (interference limited networks). This leads to the conclusion of coverage probability being independent of P.[1] Similar observations were made in [6] and [7]. However, as shown in the remaining parts of the paper, the behavior of the coverage probability with respect to λ will depend on the path loss model, and considering bounded path loss models will provide different design insights than the ones presented in [6] and [7].

Next, by using the coverage expressions presented in this section, we will focus on finding the coverage maximizing power $P^{\star}$ and BS density $\lambda^{\star}$ that solve the optimization problem posed in (2).

[1] Note that the coverage probability expressions in Lemmas 2 and 3 can be easily extended for an interference limited network by setting $\frac{1}{P} = 0$.

IV. Coverage Maximizing P and λ

The main purpose of this section is to obtain coverage maximizing (P, λ) pairs by solving the optimization problem given in (2) for general bounded path loss models. We will start by recasting the optimization problem in (2) using an equivalent format, which will facilitate the analysis. In particular, we combine the first and second constraints to obtain a new constraint $P \leq \min\left\{P_{\max}, \frac{\rho}{\lambda}\right\}$, and rewrite the optimization problem as follows.

$$\begin{array}{ll} \underset{P,\lambda}{\text{maximize}} & C_i(P,\lambda) \\ \text{subject to} & 0 \leq P \leq \min\left\{P_{\max}, \frac{\rho}{\lambda}\right\} \\ & 0 \leq \lambda \leq \lambda_{\max} \end{array}, \tag{6}$$

where $i \in \{S, N, B\}$.

As discussed in the previous section, the coverage probability expressions obtained in Lemmas 1, 2 and 3 are all strictly increasing functions of P. Therefore, any $P^\star$ solving (6) must achieve the power constraint with equality. Substituting $P = \min\left\{P_{\max}, \frac{\rho}{\lambda}\right\}$ in the objective function reduces the problem to a one dimensional constrained optimization problem without any loss of optimality. By making use of these properties, we will now focus on obtaining the coverage maximizing (P, λ) pairs. We will start with the SBCM.

A. *The* SNR*-based Coverage Model (SBCM)*

In the SBCM, $C_S(P, \lambda)$ is a strictly increasing function of λ as well (see Lemma 1). Therefore, the solution to the optimization problem will be trivial if $\lambda_{\max} P_{\max} \leq \rho$. As explained with regards to Fig. 1, the optimization problem will be independent of ρ for this scenario, and the coverage can be maximized by setting $\lambda = \lambda_{\max}$ and $P = P_{\max}$. Therefore, it is enough to only consider the case $\lambda_{\max} P_{\max} > \rho$ for the SBCM. In this case, we can trace for $\lambda^\star$ and $P^\star$ on the $P\lambda = \rho$ curve, considering $\lambda \in \left[\frac{\rho}{P_{\max}}, \lambda_{\max}\right]$ or $P \in \left[\frac{\rho}{\lambda_{\max}}, P_{\max}\right]$.

We first obtain a solution to the optimization problem of interest for the well known unbounded path loss model $g(r) = r^{-\alpha}$, which is stated in the next theorem.

Theorem 1: If $g(r) = r^{-\alpha}$ for $\alpha > 2$, $\lambda^\star = \lambda_{\max}$ and $P^\star = \frac{\rho}{\lambda_{\max}}$ solve the optimization problem in (2).

Proof: See Appendix B. ■

Theorem 1 shows that if $g(r) = r^{-\alpha}$, we end up having trivial and perhaps counter intuitive solutions to the optimization problem posed in (2), *i.e.*, the coverage probability can be maximized by maximizing the BS density in the network regardless of τ and α. If the individual constraints on P and λ are relaxed, *i.e.*, $P_{\max} = \infty$ and $\lambda_{\max} = \infty$, $C_S(P, \lambda)$ is asymptotically maximized when $\lambda \to \infty$ and $P \to 0$. This behavior is a manifestation of the unrealistic singularity at 0 in this path loss model, and can be expected to arise with any unbounded path loss model[2]. Further discussion on these flawed conclusions will be provided in Section V.

To avoid such solutions, we have assumed that the path loss model is bounded above by a constant g_0. This assumption automatically imposes a lower limit on the feasible set of transmit powers as $P \geq \frac{\tau}{g_0}$. If $P < \frac{\tau}{g_0}$, the coverage probability is zero, *i.e.*, see Definition 1. Hence, the bounded model itself imposes an implicit upper bound on the optimal λ values, thus we have $\lambda \in \left[\frac{\rho}{P_{\max}}, \min\left\{\lambda_{\max}, \frac{\rho g_0}{\tau}\right\}\right]$. This observation implies that a numerical search can be performed over a compact subset of candidate λ values on the $P\lambda = \rho$ curve to find the optimum λ and P with limited computational complexity.

In the next theorem, we show that if the path loss function satisfies some sufficient conditions in addition to the ones stated in Section II, we can further truncate the search space, and we can obtain analytical expressions for coverage maximizing λ and P values. For the clarity of presentation, we will only focus on the most interesting cases, *i.e.*, we will assume $P_{\max}\lambda_{\max} > \rho$ and $\lambda_{\max} < \frac{\rho g_0}{\tau}$. Note that the assumption on $\lambda_{\max}$ will not affect the optimization problem since the coverage probability is zero for all $\lambda \geq \frac{\rho g_0}{\tau}$. We present the coverage results for this case through the following theorem

Theorem 2: Let $g(r)$ be bounded from above, twice continuously differentiable, and satisfies $3\left(g'(r)\right)^2 \geq 2g(r)g''(r)$ for all $r \in \left[g^{-1}\left(\frac{\tau\lambda_{\max}}{\rho}\right), g^{-1}\left(\frac{\tau}{P_{\max}}\right)\right]$. If there exists a solution $r^\star$ to $r + \frac{2g(r)}{g'(r)} = 0$ such that $\lambda^\star = \frac{\rho}{\tau}g(r^\star) \in [\frac{\rho}{P_{\max}}, \lambda_{\max}]$, then it is unique, and $\lambda^\star$ maximizes the coverage probability. Otherwise, $\lambda^\star = \frac{\rho}{P_{\max}}$ or $\lambda^\star = \lambda_{\max}$. Further, the coverage probability maximizing power $P^\star$ is given by $\frac{\rho}{\lambda^\star}$.

Proof: See Appendix B. ■

The sufficient conditions given in Theorem 2 are in fact satisfied by many frequently used bounded path loss models, and an example is provided in Section V. Next, we will consider the SINR based coverage models.

B. *The* SINR*-based Coverage Models*

Obtaining coverage maximizing P and λ pairs for the SINR based models is relatively more difficult due to the complexity of the coverage probability expressions. Therefore, we will first modify the coverage probability expressions obtained in the previous section such that they represent the objective function of the optimization problem of interest more compactly, through the following lemma.

Lemma 4: Let $j \in \{1, 3\}$, $\lambda \in [0, \lambda_{\max}]$, and $\bar{q}_j$ be as given below.

$$\bar{q}_j(\lambda, r) = \begin{cases} q_j(P_{\max}, \lambda, r) & \text{if } \lambda \leq \frac{\rho}{P_{\max}} \\ q_j\left(\frac{\rho}{\lambda}, \lambda, r\right) & \text{if } \lambda \geq \frac{\rho}{P_{\max}} \end{cases}.$$

On the curve $P = \min\left\{P_{\max}, \frac{\rho}{\lambda}\right\}$, let also $C_N(\lambda)$ and $C_B(\lambda)$ be coverage probabilities as a function of λ corresponding to those obtained in Lemmas 2 and 3, respectively. Then, it is enough to replace q_j with $\bar{q}_j$, $j = 1$ and 3, to obtain $C_N(\lambda)$ and $C_B(\lambda)$, respectively.

We skip the proof since it is straightforward. According to this lemma, if $\rho \leq P_{\max}\lambda_{\max}$, there exists $\bar{\lambda} = \frac{\rho}{P_{\max}} \in (0, \lambda_{\max}]$ such that $P = P_{\max}$ for $\lambda \leq \bar{\lambda}$, and $P = \frac{\rho}{\lambda}$ for $\lambda \geq \bar{\lambda}$. Therefore, for this case, $C_N(\lambda)$ and $C_B(\lambda)$ can be visualized as a concatenation of two functions with a gluing point at $\frac{\rho}{P_{\max}}$. Also, if $\rho > P_{\max}\lambda_{\max}$, it is not hard to see that $P^\star = P_{\max}$. However, unlike the SBCM, the value of $\lambda^\star$ is not straightforward to obtain even for this particular case.

Now, we will focus on using the coverage probability expressions obtained in Lemma 4 to obtain the coverage

[2]The main focus of this paper is on the general bounded path loss models, and hence we do not discuss general unbounded path loss models any further.

maximizing transmit power and BS density for the SINR-based coverage models. Obtaining analytical expressions for $\lambda^\star$ and $P^\star$ for these two models, as we did for the SBCM, is rather complex. This because formally characterizing the behavior of $C_N(\lambda)$ and $C_B(\lambda)$ with respect to λ is difficult due to the presence of the integral over the variable representing the distance. This means the behavior of the objective function will depend on the path loss model. Moreover, the objective function is a product of a strictly increasing (*i.e.*, the $\pi\lambda$ term in front of the integral) linear function and a strictly decreasing (*i.e.*, the integral term) convex function of λ. Therefore, we need to study the behavior of the product of two convex functions. The behavior of the resulting product function cannot be generalized [26]. However, since λ is bounded by $\lambda_{\max}$, a numerical search can be performed over the compact subset of candidate λ values, to find the optimum λ with limited computational complexity.

In the next theorem, we provide further upper bounds on $\lambda^\star$ that can be used effectively in cases where $\lambda_{\max}$ is large to further decrease the time of the numerical search for finding $\lambda^\star$ and $P^\star$.

Theorem 3: Let $\lambda^\star$ and $P^\star$ be the optimal BS density and the optimal transmit power maximizing coverage probability subject to $P\lambda \leq \rho$, $\lambda \leq \lambda_{\max}$ and $P \leq P_{\max}$, respectively, for both NBCM and BBCM. Then, for $P_{\max}\lambda_{\max} < \rho$, $P^\star = P_{\max}$ and $\lambda^\star \in [0, \lambda_{\max}]$. For $P_{\max}\lambda_{\max} \geq \rho$,

$$\lambda^\star \in \begin{cases} \left[0, \min\left\{\frac{\rho g_0}{\tau}, \lambda_{\max}\right\}\right] & \text{if } P_{\max} \geq \frac{\tau}{g_0} \\ \left[0, \frac{\rho}{P_{\max}}\right] & \text{if } P_{\max} \leq \frac{\tau}{g_0} \end{cases},$$

and $P^\star = \frac{\rho}{\lambda^\star}$.

Proof: See Appendix B. ■

According to Theorem 3, the numerical search for optimizing coverage probability can be further truncated depending on the conditions given in the theorem. How large $\lambda_{\max}$ should be to truncate the search space is relative to $P_{\max}$ and ρ values. If $\lambda_{\max} \geq \frac{\rho}{P_{\max}}$, a truncation of the search space is possible. Otherwise, $\lambda_{\max}$ is already small (relative to $P_{\max}$ and ρ), and we should search over $[0, \lambda_{\max}]$ to find $\lambda^\star$. The tightness of these bounds will depend on the path loss model and the selection of $\lambda_{\max}$. It may be possible to obtain tighter bounds if the analysis is performed for a specific path loss model. The theorem will also be useful in cases where the individual constraints on λ and P are relaxed. In this case, the numerical search for optimizing coverage probability can be performed just over $\lambda \in \left[0, \frac{\rho g_0}{\tau}\right]$, thus still providing a compact subset of candidate λ values to perform the numerical search. In the next section, we will apply these results to a specific bounded path loss model to provide further insights.

Before proceeding with numerical examples, we note that the special case of the NBCM in which the distance to the nearest BS is fixed provides useful insights when the objective function does not strictly decrease with λ. For example, we can consider maximizing the average number of users covered per unit area with the same set of constraints as in (2). For a given distance, the problem can be solved by solving the equivalent optimization problem of maximizing $\lambda C_N(P, \lambda | \|x^\star\|)$ [27].

V. Applications and Numerical Evaluations

The results obtained in Sections III and IV are applicable to any bounded path loss model that satisfies the conditions given in Section II. Therefore, they can be applied to most bounded path loss models found in the literature including path loss models that are not continuously differentiable. For example, $g(r)$ can be $g(r) = \max(r_0, r)^{-\alpha}$, where r_0 is a constant that accounts for a near-field zone around each BS up to a certain distance. In this section, we will apply our results to the path loss model $g(r) = (1 + r^\alpha)^{-1}$ for $\alpha > 2$ [12], [13], [28], to provide further insights. For this model, $g_0 = 1$.

We will start with the SBCM, and will provide an application of the results in Theorem 2 through the following corollary.

Corollary 1: For the path loss model taking the form of $g(r) = (1 + r^\alpha)^{-1}$ for $\alpha > 2$, $\lambda^\star = \frac{\rho}{\tau}\left(\frac{\alpha-2}{\alpha}\right)$ maximizes the coverage probability if $\lambda^\star \in [\frac{\rho}{P_{\max}}, \lambda_{\max}]$. Otherwise, $\lambda^\star = \frac{\rho}{P_{\max}}$ or $\lambda^\star = \lambda_{\max}$. $P^\star$ is given by $\frac{\rho}{\lambda^\star}$.

Proof: See Appendix C. ■

Next, we focus on the SINR-based models, and obtain coverage probability expressions considering this specific path loss model.

Corollary 2: For the path loss model taking the form of $g(r) = (1 + r^\alpha)^{-1}$ for $\alpha > 2$, q_1 and q_3 in Lemmas 2 and 3 can be further simplified as

$$q_1(P, \lambda, r) = \frac{\tau\left(1 + r^{\frac{\alpha}{2}}\right)}{P} + \frac{2\pi\tau\left(1 + r^{\frac{\alpha}{2}}\right)\lambda}{(\alpha - 2)\, r^{\frac{\alpha}{2}-1}} \times \mathrm{GHF}\left(1, 1 - \frac{2}{\alpha}; 2 - \frac{2}{\alpha}; -\tau - \frac{(1+\tau)}{r^{\frac{\alpha}{2}}}\right) + \lambda\pi r,$$

$$q_3(P, \lambda, r) = \frac{\tau\left(1 + r^{\alpha/2}\right)}{P} + \frac{2\pi^2 \csc\left(\frac{2\pi}{\alpha}\right)\tau\left(1 + r^{\alpha/2}\right)\lambda}{\alpha\left[\tau\left(1 + r^{\alpha/2}\right) + 1\right]^{1-2/\alpha}},$$

respectively, where $\mathrm{GHF}(\cdot)$ represents the Gauss hypergeometric function [29].

Proof: See Appendix C. ■

We first present how the coverage probability behaves with λ under constraints on λ, P and $P\lambda$. We do not focus on the SNR-based coverage model for the numerical evaluations since its behavior, and the solutions to (2), can be fully characterized analytically when applied to this specific path loss model, as shown in Corollary 1. Figure 2 illustrates the behavior of the coverage probability considering the SINR-based coverage models, and for $\rho = 1$, $\alpha = 4$, $\tau = 1.1$, $\lambda_{\max} = 1.25$, and $P_{\max} = 2$. We have $P_{\max}\lambda_{\max} \geq \rho$. Therefore, as discussed in Lemma 4, the gluing point is at $\frac{\rho}{P_{\max}} = 0.5$. We can observe that for both NBCM and BBCM, the coverage maximizing λ is between zero and $\frac{\rho}{\tau}$, which is in accordance with Theorem 3. The coverage probability first increases with λ up to $\lambda^\star$ since increasing the density of the BSs decreases the average distance between a user and its associated BS. However, after $\lambda^\star$, increasing the density further will increase interference more dominantly and deteriorate the coverage probability. For this set of parameters and the selected path loss model, the coverage probability seems to be quasi-concave over λ. Therefore, in this specific instance, a common root finding algorithm can be used on

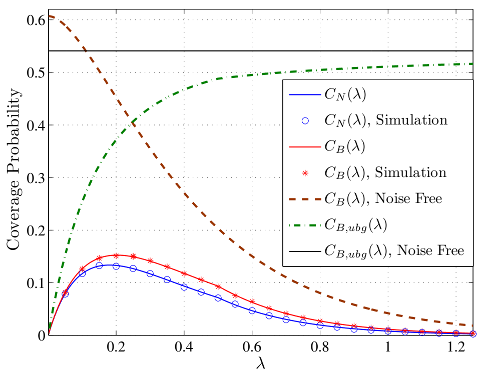

(a) $\lambda \in [0, \lambda_{\max}]$.

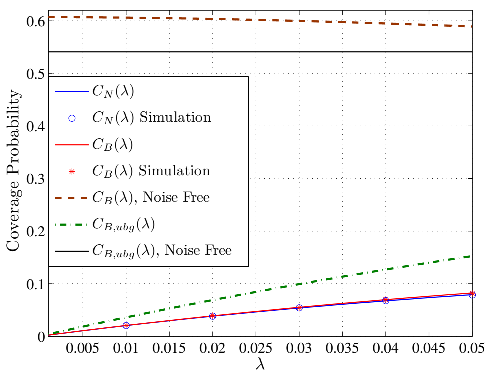

(b) $\lambda \in [0, 0.05]$.

Fig. 2. Behavior of coverage probability with λ, where $\rho = 1$, $\alpha = 4$, $\tau = 1.1$, $\lambda_{\max} = 1.25$ and $P_{\max} = 2$.

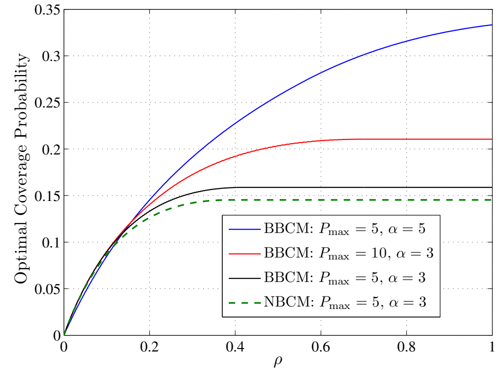

Fig. 3. The boundary between feasible and infeasible power density-coverage probability pairs for given BS density and power constraints, where $\tau = 1.1$ and $\lambda_{\max} = 1$.

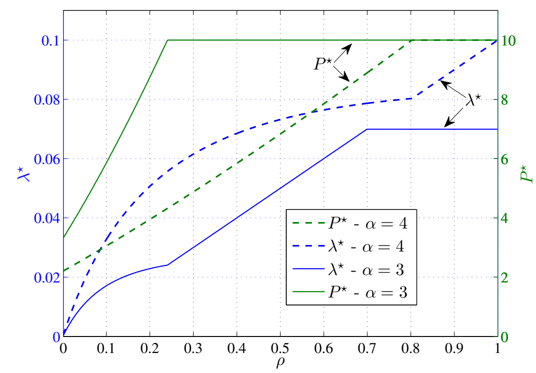

Fig. 4. The behavior of $\lambda^\star$ with the power density constraint ρ, where $\tau = 1.1$, $\lambda_{\max} = 1$ and $P_{\max} = 10$.

the first derivative of the coverage probability to find $\lambda^\star$.[3] Our bounds can be used to increase the efficiency of such a root finding procedure as well. Also, as expected, we observe that $C_B(\lambda^\star) \geq C_N(\lambda^\star)$. Simulation results are also provided to validate the coverage probability expressions obtained in Corollary 2.

Furthermore, Fig. 2 depicts the behavior of the coverage probability of the BBCM if an unbounded path loss model, $g(r) = r^{-\alpha}$, is used for the coverage analysis (denoted by $C_{B,ubg}(\lambda)$ in the figure). Similar to the result presented for the SBCM in Theorem 1, the coverage probability is strictly increasing with λ for the SINR-based models. As mentioned before, this behavior is a manifestation of the unrealistic singularity at 0 in this path loss model. Due to such a singularity, a user can progressively achieve higher channel power gains without any bound by getting closer and closer to a BS, irrespective of the interference. Therefore, maximizing the BS density in the network maximizes the coverage simultaneously, *i.e.*, when λ tends to $\lambda_{\max}$ as discussed in Theorem 1. It is also interesting to consider how the coverage probability behaves with λ in an interference limited network. Rather surprisingly, [6] and [7] showed that the coverage probability is independent of λ in interference limited networks, which can be called the *density-invariance property of outage probability*. However, this seems to be another manifestation of the aforementioned singularity. When increasing λ, the unbounded channel gains cause an increase in the strength of the useful signal to fully cancel out the increased interference power, which leads to such an invariance property. With a bounded path loss model, this invariance property can be expected to hold only for small values of λ since typical distances between transmitters and receivers in scarce wireless networks are usually large and both bounded and unbounded path loss models behave similarly for such large distances. How small the values of λ for this density invariance property to hold depends on the particular choice of the bounded path loss model. Figure 2(b), which is presented to illustrate the behavior of the coverage probability for small values of λ, clearly shows this phenomenon, and also shows that the threshold value after which the density-invariance property does not hold is rather small. Therefore, the density-invariance property of outage probability can only be expected to arise in sparse networks.

Figure 3 illustrates the change of maximum achievable coverage probability as a function of ρ for the SINR-based models. The curves, in particular, represent the boundaries between feasible and infeasible power density-coverage probability pairs for this particular path loss model. We have set $\tau = 1.1$ and $\lambda_{\max} = 1$. Consider one of the curves in the figure and a given power density constraint $\bar{\rho}$. For this power constraint, any power density-coverage probability pair below the curve can be achieved, whereas the power density-coverage probability pairs above the curve cannot be achieved. However, although being achievable, a pair strictly below the curve is sub-optimal in the sense that we can achieve a higher coverage probability while maintaining the

[3] In implementation, special consideration should be given to the point $\frac{\rho}{P_{\max}}$ since the function is not differentiable at this point.

same power density constraint $\bar{\rho}$, or we can achieve the same coverage probability with $\rho < \bar{\rho}$. Therefore, these curves can be considered as the Pareto optimal boundary between the power density constraint and the coverage probability for the system in consideration.

We can also clearly observe that the coverage probability is constant after a certain value of ρ in Fig. 3. Hence, the coverage optimization problem becomes independent of ρ after this particular value of ρ. It is interesting to note that the maximum achievable coverage probabilities increase with α, which is rather counter-intuitive at first glance. In the current setting, the signals are impaired by interference. Increasing α decreases both the received power and the interference, resulting in an upwards shift in the optimum coverage probability curves. However, when ρ is small, we can observe that the coverage probabilities decrease with α. This is because at low ρ, the SINR is noise dominated. Increasing α decreases the received power, thus reducing the SINR and the coverage probability.

Figure 4 illustrates the behavior of $\lambda^\star$ and $P^\star$ with the power density constraint ρ for the BBCM. The curves for the NBCM are similar, and therefore skipped to eliminate repetition. The plot contains two y-axis, with the one on the left representing the values for $\lambda^\star$, and the one on the right representing the values for $P^\star$. We will use the $\alpha = 3$ curves for the explanations below, and we have $\tau = 1.1$, $\lambda_{\max} = 1$ and $P_{\max} = 10$. We can observe that both $\lambda^\star$ and $P^\star$ increase nonlinearly with ρ up to $\lambda^\star = \frac{\rho}{P_{\max}}$, which is the point where $P^\star$ reaches the limit $P_{\max}$. When ρ is further increased, $\lambda^\star$ increases linearly with ρ with a slope of $\frac{1}{P_{\max}}$, and then becomes independent of ρ. Note that the value of ρ at which $\lambda^\star$ becomes independent of ρ, and the value of ρ at which the optimal coverage probability becomes independent of ρ, which is illustrated in Fig. 3, coincide. It is interesting to note that unlike the SBCM case, $\lambda^\star$ becomes independent of ρ before ρ exceeds $P_{\max}\lambda_{\max}$. This is because, for the SBCM, the coverage was a strictly increasing function of both λ and P as shown in Lemma 1. For this particular scenario on the other hand, it is a strictly increasing function of P, but not over λ as shown in Fig. 2. This observation has the important ramification that, after some value of ρ, there is no benefit of increasing λ excessively for the purposes of coverage maximization, because interference in the network also increases with denser BS deployment. The system would do better by increasing P instead, but in this particular case, it has already fully utilized the power resources. These explanations can also be used to deduce the behavior of $\lambda^\star$ and $P^\star$ if $\lambda_{\max}$ is set at a very small value, *i.e.*, $\lambda^\star$ reaches $\lambda_{\max}$ before $P^\star$ reaches $P_{\max}$ (plots are not provided to avoid repetition). For this case, $\lambda^\star$ and $P^\star$ will increase nonlinearly with ρ up to $\lambda^\star = \lambda_{\max}$, after which $\lambda^\star$ will become independent of ρ. However, since the coverage is strictly increasing with P, $P^\star$ will increase linearly with ρ with a slope of $\frac{1}{\lambda_{\max}}$ until it reaches $P_{\max}$. Finally, Fig. 4 shows that $\lambda^\star$ increases with α. This is because both interference and transmitted signal power decay more rapidly at higher values of α.

The behavior of $\lambda^\star$ with ρ can also be explained with further insights by using the behavior of $C_B(\lambda)$. We set $\tau = 1.1$, $\alpha = 3$, $\lambda_{\max} = 1$ and $P_{\max} = 10$ in Fig. 5.

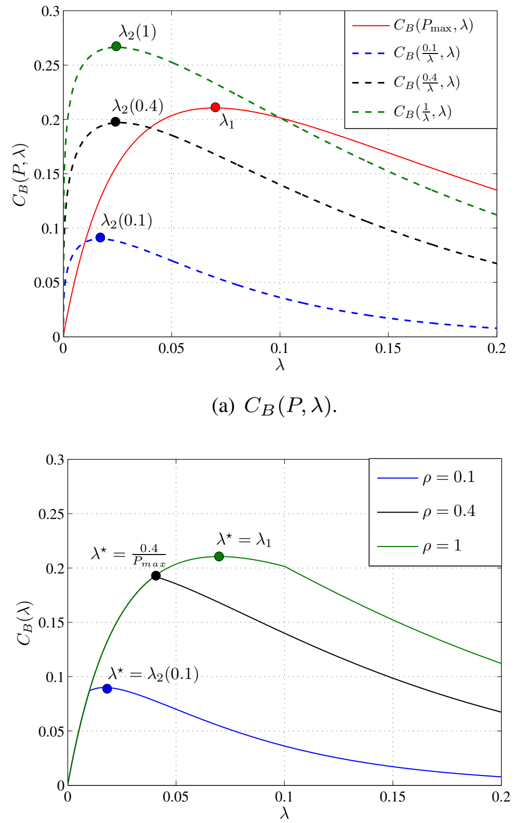

Fig. 5. The behavior of coverage probability with λ for different power density constraints ρ, where $\tau = 1.1$, $\alpha = 3$, $\lambda_{\max} = 1$ and $P_{\max} = 10$.

As explained in Lemma 4, the behavior of $C_B(\lambda)$ can be visualized as the concatenation of two functions with a gluing point at $\frac{\rho}{P_{\max}}$, *i.e.*, $C_B(\lambda) \triangleq C_B(P_{\max}, \lambda)$ if $\lambda \leq \frac{\rho}{P_{\max}}$, and $C_B(\lambda) \triangleq C_B(\frac{\rho}{\lambda}, \lambda)$ if $\lambda > \frac{\rho}{P_{\max}}$. In Fig. 5(a), we illustrate the behavior of $C_B(\frac{\rho}{\lambda}, \lambda)$ with λ for three different values of ρ, and the behavior of $C_B(P_{\max}, \lambda)$, which is independent of ρ. For a particular value of ρ, the gluing point, *i.e.*, $\lambda = \frac{\rho}{P_{\max}}$, is the intersection point of $C_B(\frac{\rho}{\lambda}, \lambda)$ and $C_B(P_{\max}, \lambda)$. The resulting $C_B(\lambda)$ curves are presented in Fig. 5(b). For an example, if $\rho = 0.1$, $C_B(\lambda)$ will be represented by the red $C_B(P_{\max}, \lambda)$ line in Fig. 5(a) for values of $\lambda \in \left[0, \frac{0.1}{P_{\max}}\right]$, and will be represented by the blue dashed line elsewhere, as shown in Fig. 5(b). Let λ_1 be the value of λ that maximizes $C_B(P_{\max}, \lambda)$, and let $\lambda_2(\rho)$ be the value of λ that maximizes $C_B(\frac{\rho}{\lambda}, \lambda)$. Now let us focus on the behavior of $C_B(\lambda)$. As shown in Fig. 5(a) for $\rho = 0.1$ case, when ρ is small, $\lambda_2(\rho)$ will be the coverage maximizing λ, which increases with ρ. This behavior can be observed for all values of ρ that satisfy $\frac{\rho}{P_{\max}} \leq \lambda_2(\rho)$. However, if $\lambda_2(\rho) \leq \frac{\rho}{P_{\max}} \leq \lambda_1$, we have $\lambda^\star = \frac{\rho}{P_{\max}}$, as shown in the figure for $\rho = 0.4$. Therefore, $\lambda^\star$ increases linearly with ρ within this interval, which can also be observed in Fig. 4. When $\lambda_1 \leq \frac{\rho}{P_{\max}}$, $\lambda^\star = \lambda_1$ as shown in the figure for $\rho = 1$. Therefore, $\lambda^\star$ will be independent of ρ for all $\rho > P_{\max}\lambda_1$.

VI. Conclusions

In this paper, we have studied the coverage probability maximization problem for Poisson cellular networks, under constraints on the transmit power P, BS density λ, and power density $P\lambda$. We have considered three coverage models that differ from each other depending on the metric used to decide whether a user is in coverage or not. The first model is based on the received unfaded SNR at a user, and the other two models that have different user-BS association rules are based on the users' received instantaneous SINR. We have obtained coverage probability expressions using stochastic geometry for each of these models. Firstly, we have solved the optimization problem analytically considering the SNR-based coverage model, where interference and random fading effects are neglected. In particular, we have shown that using unbounded path loss models to characterize the location dependent path loss values of the users will lead to trivial solutions. We have then focused on the SINR-based coverage models, considering general bounded path loss models. To this end, we have shown how the optimization problem can be reduced to a constrained single dimensional optimization problem over λ without any loss of optimality, and we have resorted to a numerical search over a compact subset of candidate λ values to find the optimum λ. We have further truncated the search space by providing more tighter bounds on λ. Finally, we have applied the derived results to a specific bounded path loss model to obtain further insights. In particular, we have illustrated how the coverage probability behaves for different system parameters and the constraints, and how the coverage maximizing λ and P values change when the constraint on power density is relaxed. The plots show that although the coverage can be improved indefinitely by increasing P, the coverage becomes interference limited and it cannot be improved indefinitely by increasing λ. On the other hand, if the path loss model is unbounded, the coverage probability can be improved indefinitely by increasing λ, which is a manifestation of the unrealistic singularity at 0 in this path loss model. We have also illustrated the Pareto optimal boundary between the power density constraint and the coverage probability for given $\lambda_{\max}$ and $P_{\max}$. Any power density-coverage probability pair below the curve is achievable, but suboptimal, whereas any power density-coverage probability pair above the curve cannot be achieved.

Appendix A
Coverage Probability Calculations

A. SBCM: Proof of Lemma 1

We have

$$C_S(P,\lambda) = \mathsf{Pr}\left\{Pg(\|x^\star\|) > \tau\right\} = \mathsf{Pr}\left\{\|x^\star\| \le g^{-1}\left(\frac{\tau}{P}\right)\right\}$$

since g is non-increasing. Also, since the BS locations are modeled as a PPP, the cumulative distribution function (CDF) of $\|x^\star\|$ can be written as

$$F_{\|x^\star\|}(r) = 1 - \mathrm{e}^{-\lambda\pi r^2}, \tag{7}$$

by using the null probability for PPPs [4]. Therefore, $\mathsf{Pr}\left\{\|x^\star\| \le g^{-1}\left(\frac{\tau}{P}\right)\right\} = 1 - \mathrm{e}^{-\lambda\pi\left(g^{-1}\left(\frac{\tau}{P}\right)\right)^2}$, which completes the proof.

B. NBCM: Proof of Lemma 2

We will first consider the distance to the nearest BS to be given. Then, we have $C_N(P,\lambda|\,\|x^\star\|) = \mathsf{Pr}\left\{\frac{Ph_{x^\star}g(\|x^\star\|)}{1+I} > \tau \middle| \|x^\star\|\right\}$, where I represents the interference term in (1). By conditioning on I, and by using the fact that fading gains are unit exponential distributed,

$$\begin{aligned} C_N(P,\lambda|\,\|x^\star\|) &= \mathsf{E}_I\left[\mathsf{Pr}\left\{h_{x^\star} > \frac{\tau(1+I)}{Pg(\|x^\star\|)}\middle| I, \|x^\star\|\right\}\right] \\ &= \mathrm{e}^{\frac{-\tau}{Pg(\|x^\star\|)}}\mathsf{E}_I\left[\mathrm{e}^{\frac{-\tau I}{Pg(\|x^\star\|)}}\right]. \end{aligned} \tag{8}$$

Since fading gains are i.i.d. and independent of Φ, we have

$$\begin{aligned} \mathsf{E}_I\left[\mathrm{e}^{\frac{-\tau I}{Pg(\|x^\star\|)}}\right] &= \mathsf{E}_\Phi\left[\prod_{y\in\Phi\setminus\{x^\star\}}\mathsf{E}_h\left[\mathrm{e}^{\frac{-\tau hg(\|y\|)}{g(\|x^\star\|)}}\right]\right] \\ &= \mathsf{E}_\Phi\left[\prod_{y\in\Phi\setminus\{x^\star\}}\frac{g(\|x^\star\|)}{g(\|x^\star\|)+\tau g(\|y\|)}\right]. \end{aligned}$$

We note that $\Phi' = \Phi\setminus\{x^\star\}$ is a PPP on $\mathbb{R}^2\setminus B(0,\|x^\star\|)$, where $B(0,r)$ represents a disk centered at the origin with radius r. By using the probability generating functional for PPPs,

$$\mathsf{E}_I\left[\mathrm{e}^{\frac{-\tau I}{Pg(\|x^\star\|)}}\right] = \mathrm{e}^{-\lambda\int_{\mathbb{R}^2\setminus B(0,\|x^\star\|)}\left(1-\frac{g(\|x^\star\|)}{g(\|x^\star\|)+\tau g(\|y\|)}\right)dy}.$$

By changing the coordinates from cartesian to polar and evaluating the resulting integration over the area of the interfering BSs, we have

$$\mathsf{E}_I\left[\mathrm{e}^{\frac{-\tau I}{Pg(\|x^\star\|)}}\right] = \exp\left(-\lambda\int_{\|x^\star\|}^{\infty}\frac{2\pi\tau t g(t)}{g(\|x^\star\|)+\tau g(t)}dt\right).$$

Using the final expression obtained for $\mathsf{E}_I\left[\mathrm{e}^{\frac{-\tau I}{Pg(\|x^\star\|)}}\right]$ in (8) with a change of variables $t^2 = v$ gives us $C_N(P,\lambda|\,\|x^\star\|) = \exp\left(-q_2(P,\lambda,\|x^\star\|)\right)$.

Then, we have

$$\begin{aligned} C_N(P,\lambda) &= \int_0^\infty C_N(P,\lambda|t)dF_{\|x^\star\|}(t) \\ &= 2\lambda\pi\int_0^\infty t\exp\left(-\lambda\pi t^2 - q_2(P,\lambda,t)\right)dt. \end{aligned}$$

A change of variables $t^2 = r$ completes the proof.

C. BBCM: Proof of Lemma 3

Since $\tau > 1$, we have

$$C_B(P,\lambda) = \sum_{x\in\Phi}\mathsf{Pr}\left\{\mathrm{SINR}_x > \tau\right\} = \mathsf{E}\left[\sum_{x\in\Phi}1_{\{\mathrm{SINR}_x>\tau\}}\right].$$

Then, by using Campbell-Mecke Theorem [4],

$$C_B(P,\lambda) = \lambda\int_{\mathbb{R}^2}\mathsf{Pr}\left\{\frac{Ph_xg(\|x\|)}{1+I} > \tau\right\}dx,$$

where I represents the interference term in (1). Making a coordinate change from cartesian to polar, and by using Lemma 2, we can write

$$\begin{aligned} C_B(P,\lambda) &= 2\pi\lambda\int_0^\infty\mathsf{Pr}\left\{\frac{Ph_xg(r)}{1+I} > \tau\middle| \|x\| = r\right\}rdr \\ &= 2\pi\lambda\int_0^\infty\mathrm{e}^{\frac{-\tau}{Pg(r)}}\mathsf{E}_I\left[\mathrm{e}^{\frac{-\tau I}{Pg(r)}}\right]rdr. \end{aligned}$$

Evaluation of $\mathsf{E}_I\left[\mathrm{e}^{\frac{-\tau I}{Pg(r)}}\right]$ is similar to what we have done in the proof of Lemma 2, with the only difference being in the limits of the integration because the interfering BSs can now be located anywhere in the plane, *i.e.*, the integration is from 0 to ∞, which completes the proof.

APPENDIX B
SOLUTIONS TO THE OPTIMIZATION PROBLEM

A. SBCM with an Unbounded Path Loss Model: Proof of Theorem 1

From Lemma 1, we have

$$C_S(\lambda) = 1 - \mathrm{e}^{-\pi\left(\frac{\rho}{\tau}\right)^{\frac{2}{\alpha}}\lambda^{1-\frac{2}{\alpha}}}$$

for $P = \frac{\rho}{\lambda}$. This is clearly a strictly increasing function of λ since $\alpha > 2$. Therefore, coverage is maximized by setting $\lambda = \lambda_{\max}$ and $P = \frac{\rho}{\lambda_{\max}}$, which completes the proof.

B. SBCM with a Bounded Path Loss Models: Proof of Theorem 2

Since we are tracing values on the $P\lambda = \rho$ curve, $P = \frac{\rho}{\lambda}$ and

$$C_S(\lambda) \triangleq C_S(\frac{\rho}{\lambda}, \lambda) = 1 - \mathrm{e}^{-\lambda\pi\left(g^{-1}\left(\frac{\tau\lambda}{\rho}\right)\right)^2}.$$

Let $f(\lambda) = \lambda\left(g^{-1}\left(\frac{\tau\lambda}{\rho}\right)\right)^2$. Maximizing $C_S(\lambda)$ is equivalent to maximizing $f(\lambda)$. By differentiating $f(\lambda)$ with respect to λ, we get $f'(\lambda) = g^{-1}\left(\frac{\tau\lambda}{\rho}\right)q(\lambda)$, where

$$q(\lambda) = g^{-1}\left(\frac{\tau\lambda}{\rho}\right) + \frac{2\lambda\tau}{\rho g'\left(g^{-1}\left(\frac{\tau\lambda}{\rho}\right)\right)}.$$

Let $g^{-1}\left(\frac{\tau\lambda}{\rho}\right) = r$. Since $\lambda \in \left[\frac{\rho}{P_{\max}}, \lambda_{\max}\right]$, we have $r \in \left[g^{-1}\left(\frac{\tau\lambda_{\max}}{\rho}\right), g^{-1}\left(\frac{\tau}{P_{\max}}\right)\right]$. Therefore, if a solution $r^\star$ to $q(r) = r + \frac{2g(r)}{g'(r)} = 0$ exists, $\lambda^\star = \frac{\rho}{\tau}g(r^\star)$ gives us the critical values of λ that maximize $f(\lambda)$.

Now, by differentiating $q(\lambda)$ with respect to λ,

$$q'(\lambda) = \frac{\tau}{\rho g'\left(g^{-1}\left(\frac{\tau\lambda}{\rho}\right)\right)}\left[3 - \frac{2\lambda\tau}{\rho}\frac{g''\left(g^{-1}\left(\frac{\tau\lambda}{\rho}\right)\right)}{\left(g'\left(g^{-1}\left(\frac{\tau\lambda}{\rho}\right)\right)\right)^2}\right]. \tag{9}$$

The term in the parenthesis in (9) can be replaced by $t(r) = 3 - 2g(r)\frac{g''(r)}{g'(r)}$. We have $t(r) \geq 0$ since $3\left(g'(r)\right)^2 \geq 2g(r)g''(r)$ for all r in the region of interest. Therefore, $q'(\lambda) \leq 0$, implying that $q(\lambda)$ is strictly decreasing with λ for $\lambda \in \left[\frac{\rho}{P_{\max}}, \lambda_{\max}\right]$.

Now, we will consider three different cases. Firstly, if $q(\frac{\rho}{P_{\max}}) \leq 0$, $q(\lambda) \leq 0$ for all $\lambda \in \left[\frac{\rho}{P_{\max}}, \lambda_{\max}\right]$. Thus, $\lambda = \frac{\rho}{P_{\max}}$ maximizes $f(\lambda)$. Secondly, if $q(\lambda_{\max}) \geq 0$, $q(\lambda) \geq 0$ for all $\lambda \in \left[\frac{\rho}{P_{\max}}, \lambda_{\max}\right]$. Thus, $\lambda = \lambda_{\max}$ maximizes $f(\lambda)$. Finally, if $q(\frac{\rho}{P_{\max}}) \geq 0$ and $q(\lambda_{\max}) \leq 0$, then there exists a unique critical value $\lambda^\star = \frac{\rho}{\tau}g(r^\star)$ that makes $q(\lambda^\star) = 0$, and thus maximizes $f(\lambda)$.

C. NBCM and BBCM: Proof of Theorem 3

We will only give the proof for the NBCM. The proof for the BBCM follows from similar lines, and hence, is omitted. Directly from the constraints in (2), we have $\lambda^\star \in [0, \lambda_{\max}]$ for $P_{\max}\lambda_{\max} < \rho$, and $P^\star = P_{\max}$ since the coverage probability is strictly increasing with P.

Now we will consider $P_{\max}\lambda_{\max} \geq \rho$, which leads to a tradeoff between P and λ. We will first study the behavior of the objective function on the curve $P = \frac{\rho}{\lambda}$. For this case, $C_N(\lambda)$ takes the form of

$$C_N(\lambda) = \pi\lambda\int_0^\infty \exp\left(-\lambda\left(\tilde{q}(r) + \frac{\tau}{\rho g(\sqrt{r})}\right)\right)dr,$$

where $\tilde{q}(r)$ is a positive function of r. By differentiating with respect to λ, we have

$$C_N'(\lambda) = \pi\int_0^\infty \mathrm{e}^{-\lambda\left(\tilde{q}(r)+\frac{\tau}{\rho g(\sqrt{r})}\right)}\left[1 - \frac{\lambda\tau}{\rho g(\sqrt{r})} - \lambda\tilde{q}(r)\right]dr,$$

which is strictly negative if $\frac{\lambda\tau}{\rho g_0} \geq 1$. Therefore, $C_N(\lambda)$ is strictly decreasing for all $\lambda \geq \frac{\rho g_0}{\tau}$.

If $P_{\max}\lambda_{\max} \geq \rho$, we have $P = \frac{\rho}{\lambda}$ for all $\lambda \geq \frac{\rho}{P_{\max}}$. We have already shown that the coverage probability on the curve $P = \frac{\rho}{\lambda}$ is strictly decreasing for all $\lambda \geq \frac{\rho g_0}{\tau}$. Therefore, if $\frac{\rho}{P_{\max}} \geq \frac{\rho g_0}{\tau}$, we have $\lambda^\star \in \left[0, \frac{\rho}{P_{\max}}\right]$. Similarly, if $\frac{\rho}{P_{\max}} \leq \frac{\rho g_0}{\tau}$, we have $\lambda^\star \in \left[0, \min\left\{\frac{\rho g_0}{\tau}, \lambda_{\max}\right\}\right]$, which completes the proof.

APPENDIX C
APPLICATIONS TO SPECIFIC PATH LOSS MODELS

A. SBCM: Proof of Corollary 1

The proof is a direct application of the results obtained in Theorem 2. To start with, $g(r) = (1 + r^\alpha)^{-1}$ is twice continuously differentiable, and bounded above by one. We have $g'(r) = -\alpha r^{\alpha-1}\left(g(r)\right)^2$, and $g''(r) = -\frac{g'(r)}{r}\left[2\alpha r^\alpha g(r) - (\alpha - 1)\right]$. Therefore,

$$3 - 2\frac{g(r)g''(r)}{\left(g'(r)\right)^2} = 1 - \frac{2}{\alpha} + \frac{1}{r^\alpha}\left(2 - \frac{2}{\alpha}\right) > 0.$$

A unique solution to $r + \frac{2g(r)}{g'(r)} = 0$ exists, and it can be simplified as $r^\star = \left(\frac{2}{\alpha-2}\right)^{\frac{1}{\alpha}}$. Thus, $\lambda^\star = \frac{\rho}{\tau}g(r^\star) = \frac{\rho}{\tau}\left(\frac{\alpha-2}{\alpha}\right)$ if $\lambda^\star \in \left[\frac{\rho}{P_{\max}}, \lambda_{\max}\right]$.

B. NBCM and BBCM: Proof of Corollary 2

For $g(r) = (1 + r^\alpha)^{-1}$, from Lemma 2, we have

$$q_2(P, \lambda, r) = \frac{\tau\left(1 + r^\alpha\right)}{P} + \lambda\pi\tau\left(1 + r^\alpha\right)\int_{r^2}^\infty \frac{1}{1 + v^{\frac{\alpha}{2}} + \tau\left(1 + r^\alpha\right)}dv.$$

A variable change $v^{\frac{\alpha}{2}} = t$ gives us

$$q_2(P, \lambda, r) = \frac{\tau\left(1 + r^\alpha\right)}{P} + \lambda\pi\tau\left(1 + r^\alpha\right)\frac{2}{\alpha\beta_1}\int_{r^\alpha}^\infty \frac{t^{\frac{2}{\alpha}-1}}{1 + \frac{t}{\beta_1}}dt,$$

where $\beta_1 = \tau\left(1 + r^\alpha\right) + 1$. Simplifying the integration using the table of integrals leads to the required expression for q_1 [29].

Similarly, by using Lemma 3 and the same variable change, we have

$$q_3(P,\lambda,r) = \frac{\tau\left(1+r^{\frac{\alpha}{2}}\right)}{P} + \lambda\pi\tau\left(1+r^{\frac{\alpha}{2}}\right)\frac{2}{\alpha\beta_2}\int_0^\infty \frac{t^{\frac{2}{\alpha}-1}}{1+\frac{t}{\beta_2}}dt,$$

where $\beta_2 = \tau\left(1+r^{\frac{\alpha}{2}}\right)+1$. Simplifying the integration using the table of integrals completes the proof.

References

[1] R. Jain, S.-I. Chakchai, and A.-K. A. Tamimi, "System-level modeling of IEEE 802.16E mobile WIMAX networks: key issues," *IEEE Wireless Commun.*, vol. 15, pp. 73–79, Oct. 2008.

[2] R. S. Karlsson, "Radio resource sharing and capacity of some multiple access methods in hierarchical cell structures," in *Proc. 1999 IEEE Vehicular Technology Conference – Fall*, pp. 2825–2829.

[3] M. Haenggi, J. G. Andrews, F. Baccelli, O. Dousse, and M. Franceschetti, "Stochastic geometry and random graphs for the analysis and design of wireless networks," *IEEE J. Sel. Areas Commun.*, vol. 27, pp. 1029–1046, Sep. 2009.

[4] M. Haenggi, *Stochastic Geometry for Wireless Networks*. Cambridge University Press, 2012.

[5] H. ElSawy, E. Hossain, and M. Haenggi, "Stochastic geometry for modeling, analysis, and design of multi-tier and cognitive cellular wireless networks: a survey," *IEEE Commun. Surveys and Tutorials*, vol. 15, pp. 996–1019, Jul. 2013.

[6] J. G. Andrews, F. Baccelli, and R. K. Ganti, "A tractable approach to coverage and rate in cellular networks," *IEEE Trans. Commun.*, vol. 59, pp. 3122–3134, Nov. 2011.

[7] H. S. Dhillon, R. K. Ganti, F. Baccelli, and J. G. Andrews, "Modeling and analysis of K-tier downlink heterogeneous cellular networks," *IEEE J. Sel. Areas Commun.*, vol. 30, pp. 550–560, Apr. 2012.

[8] H.-S. Jo, Y. J. Sang, P. Xia, and J. G. Andrews, "Heterogeneous cellular networks with flexible cell association: a comprehensive downlink SINR analysis," *IEEE Trans. Wireless Commun.*, vol. 11, pp. 3484–3495, Oct. 2012.

[9] V. Chandrasekhar, M. Kountouris, and J. G. Andrews, "Coverage in multi-antenna two-tier networks," *IEEE Trans. Wireless Commun.*, vol. 8, pp. 5314–5327, Oct. 2009.

[10] V. Chandrasekhar and J. G. Andrews, "Spectrum allocation in tiered cellular networks," *IEEE Trans. Commun.*, vol. 57, pp. 3059–3068, Oct. 2009.

[11] T. D. Novlan, H. S. Dhillon, and J. G. Andrews, "Analytical modeling of uplink cellular networks," *IEEE Trans. Wireless Commun.*, vol. 12, pp. 2669–2679, Jun. 2013.

[12] H. Inaltekin, M. Chiang, H. V. Poor, and S. B. Wicker, "On unbounded path-loss models: effects of singularity on wireless network performance," *IEEE J. Sel. Areas Commun.*, vol. 27, pp. 1078–1092, Sep. 2009.

[13] H. Inaltekin, "Gaussian approximation for the wireless multi-access interference distribution," *IEEE Trans. Signal Process.*, vol. 60, pp. 6114–6120, Nov. 2012.

[14] R. W. Heath and M. Kountouris, "Modeling heterogeneous network interference with using Poisson point processes," *IEEE Trans. Signal Process.*, vol. 61, pp. 4114–4126, May 2013.

[15] K. Huang, J. G. Andrews, D. Guo, R. W. Heath, and R. A. V. Berry, "Spatial interference cancellation for multiantenna mobile ad hoc networks," *IEEE Trans. Inf. Theory*, vol. 58, pp. 1660–1676, Oct. 2012.

[16] Z. Sheng, D. L. Goeckel, K. K. Leung, and Z. Ding, "A stochastic geometry approach to transmission capacity in wireless cooperative networks," in *Proc. 2009 International Symposium on Personal, Indoor and Mobile Radio Communications*, pp. 622–626.

[17] J. Hoydis, A. Muller, R. Couillet, and M. Debbah, "Analysis of multicell cooperation with random user locations via deterministic equivalents," in *Proc. 2012 International Symposium on Modeling and Optimization in Mobile, Ad Hoc and Wireless Networks*, pp. 374–379.

[18] X. Zhang and M. Haenggi, "Random power control in Poisson networks," *IEEE Trans. Commun.*, vol. 60, pp. 2602–2611, Sep. 2012.

[19] D. Cao, S. Zhou, and Z. Niu, "Optimal base station density for energy-efficient heterogeneous cellular networks," in *Proc. 2012 International Conference on Communications*, pp. 4379–4383.

[20] Y. S. Soh, T. Q. S. Quek, M. Kountouris, and H. Shin, "Energy efficient heterogeneous cellular networks," *IEEE J. Sel. Areas Commun.*, vol. 31, pp. 840–850, May 2013.

[21] F. Baccelli, B. Blaszczyszyn, and P. Muhlethaler, "Stochastic analysis of spatial and opportunistic ALOHA," *IEEE J. Sel. Areas Commun.*, vol. 27, pp. 1105–1119, Sep. 2009.

[22] C.-H. Lee and M. Haenggi, "Interference and outage in Poisson cognitive networks," *IEEE Trans. Wireless Commun.*, vol. 11, pp. 1536–1276, Apr. 2010.

[23] M. Sharif and B. Hassibi, "On the capacity of MIMO broadcast channels with partial side information," *IEEE Trans. Inf. Theory*, vol. 51, pp. 506–522, Feb. 2005.

[24] T. Samarasinghe, H. Inaltekin, and J. S. Evans, "Optimal selective feedback policies for opportunistic beamforming," *IEEE Trans. Inf. Theory*, vol. 59, pp. 2897–2913, May 2013.

[25] T. Samarasinghe, H. Inaltekin, and J. S. Evans, "The feedback-capacity tradeoff for opportunistic beamforming under optimal user selection," *Performance Evaluation*, vol. 70, pp. 472–492, Jul. 2013.

[26] S. Boyd and L. Vandenberghe, *Convex Optimization*. Cambridge University Press, 2004.

[27] T. Samarasinghe, H. Inaltekin, and J. S. Evans, "Maximizing the coverage-intensity product in random cellular networks," in *Proc. 2014 Australian Communications Theory Workshop.*

[28] T. Samarasinghe, H. Inaltekin, and J. S. Evans, "Outage capacity of opportunistic beamforming with random user locations," in *Proc. 2013 IEEE Global Telecommunications Conference.*

[29] I. Gradshteyn and I. Ryzhik, *Table of Integrals, Series, and Products*, 7th ed. Academic Press, 2007.

Tharaka Samarasinghe (S'11–M'13) was born in Colombo, Sri Lanka, in 1984. He received the B.Sc. degree in engineering from the Department of Electronics and Telecommunication Engineering, University of Moratuwa, Sri Lanka, in 2008, where he received the award for the most outstanding undergraduate upon graduation. He received the Ph.D. degree from the Department of Electrical and Electronic Engineering, University of Melbourne, Australia, in 2012. He has been with the Department of Electrical and Computer Systems Engineering, Monash University, Australia, since September 2012, where he is currently a research fellow. His research interests are in communications theory, information theory, and wireless communications networks.

Hazer Inaltekin (S'04–M'06) is an Associate Professor of Electrical and Electronics Engineering at Antalya International University. He received his B.S. degree (High Hons) in electrical and electronics engineering from Bogazici University, Istanbul, Turkey, in 2001, and his M.S./Ph.D. degree in electrical and computer engineering from Cornell University, Ithaca, NY, in 2006. He was a Postdoctoral Research Associate at Cornell University from 2006 to 2007, and at Princeton University, Princeton, NJ, from 2007 to 2009. In 2009, he joined the Department of Electrical and Electronic Engineering at the University of Melbourne as a Research Fellow. He was a Senior Research Fellow at the same department between January 2011 and August 2011. Since August 2011, he has been on the faculty at Antalya International University. His research interests include wireless communications, wireless networks, social networks, game theory, and information theory.

Jamie Evans (S'93–M'98) was born in Newcastle, Australia, in 1970. He received the B.S. degree in physics and the B.E. degree in computer engineering from the University of Newcastle, in 1992 and 1993, respectively, where he received the University Medal upon graduation. He received the M.S. and the Ph.D. degrees from the University of Melbourne, Australia, in 1996 and 1998, respectively, both in electrical engineering, and was awarded the Chancellors Prize for excellence for his Ph.D. thesis. From March 1998 to June 1999, he was a Visiting Researcher in the Department of Electrical Engineering and Computer Science, University of California, Berkeley. He returned to Australia to take up a position as Lecturer at the University of Sydney, Australia, where he stayed until July 2001. From July 2001 until March 2012 he was with the Department of Electrical and Electronic Engineering, University of Melbourne. He is currently a Professor in the Department of Electrical and Computer Systems Engineering at Monash University, Australia. His research interests are in communications theory, information theory, and statistical signal processing with a focus on wireless communications networks.